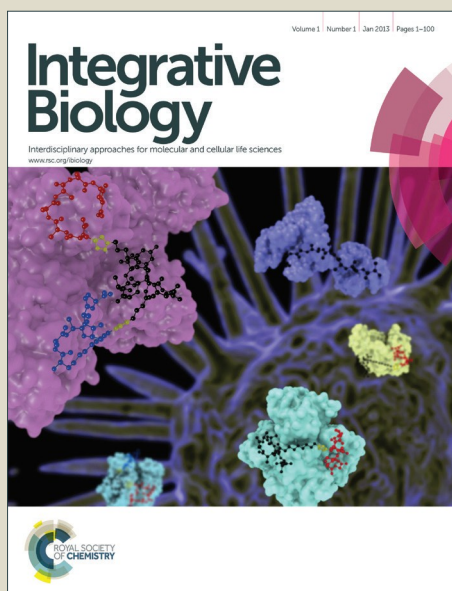


Integrative Biology

Accepted Manuscript



This is an *Accepted Manuscript*, which has been through the Royal Society of Chemistry peer review process and has been accepted for publication.

Accepted Manuscripts are published online shortly after acceptance, before technical editing, formatting and proof reading. Using this free service, authors can make their results available to the community, in citable form, before we publish the edited article. We will replace this *Accepted Manuscript* with the edited and formatted *Advance Article* as soon as it is available.

You can find more information about *Accepted Manuscripts* in the [Information for Authors](#).

Please note that technical editing may introduce minor changes to the text and/or graphics, which may alter content. The journal's standard [Terms & Conditions](#) and the [Ethical guidelines](#) still apply. In no event shall the Royal Society of Chemistry be held responsible for any errors or omissions in this *Accepted Manuscript* or any consequences arising from the use of any information it contains.

Insight Box

Secreted proteins are critical for orchestrating behaviors of cell populations, but their detection relies largely on methods that require bulk cell cultures. This study describes a technique that allows measurement of proteins secreted from individual cells cultured within adhesive microwells. We utilize this tool to examine cytokines secreted from macrophages on adhesive substrates, and with controlled geometries. Our study reveals that adhesion to extracellular matrix enhances individual cell secretion, as well as population heterogeneity. In addition, we demonstrate using microwells of different geometries that cell elongation inhibits inflammatory cytokine secretion. Together, we describe an adhesive microwell system to detect secreted products from individual cells, and provide insight to the regulation of macrophage cytokine secretion by cell adhesion and shape.

Macrophage secretion heterogeneity in engineered microenvironments revealed using a microwell platform

Frances Y. McWhorter^{a,c}, Tim D. Smith^{a,c}, Thuy U. Luu^{c,d}, Maha K. Rahim^a, Jered B. Haun^{a,b} and Wendy F. Liu^{a,b,c,*}

^aDepartment of Biomedical Engineering

^bDepartment of Chemical Engineering and Materials Science

^cThe Edwards Lifesciences Center for Advanced Cardiovascular Technology

^dDepartment of Pharmacological Sciences

University of California Irvine

2412 Engineering Hall

Irvine, CA 92697

Tel: (949) 824-1682

Fax: (949) 824-9968

Email: wendy.liu@uci.edu

* To whom correspondence may be addressed.

Abstract

Secreted proteins play a major role in orchestrating the response of cell populations. However, a quantitative understanding of the dynamic changes in protein secretion in response to microenvironmental cues at the single cell level remains elusive. Measurements taken using traditional molecular techniques typically require bulk cultures, and therefore cannot capture the diversity within cell populations. Recent advances in chip-based technologies have shown that single cell measurements can provide important insights into the temporal dynamics of cellular activation and function, but these tools have had limited control of the adhesive cellular microenvironment. Here, we created a single cell cytokine detection platform that allows for controlled physical and adhesive microenvironment. We validated the platform by examining cytokine secretion of macrophages exposed to varying dosages of soluble stimulation and on different adhesive substrates. We also used the platform to demonstrate that cell shape affects single macrophage cytokine secretion. Together, these results show the ability of the microwell system to detect secreted cytokines from individual macrophages in controlled adhesive environments. This technique may be broadly applied to detect secreted products from any adherent cell type.

Keywords: Single cell, cytokine secretion, cell adhesion, macrophage

Introduction

Secreted proteins are a critical component of cell function, as they play an important role in coordinating the response of cell populations within tissues. For the immune system, which relies on a complex network of cells that interact through densely overlapping connections and result in coordinated responses, quantitative measurements of secreted products provides an important assessment of their function. However, an intrinsic challenge to understanding immune regulation is that many immune cells, or leukocytes, can be further subcategorized based on lineages, differentiation, phenotypic, and functional states.¹ Clinical samples of single immune cell type show remarkable heterogeneity and present distinct phenotypic (cell surface or intracellular markers), functional (secreted products), and genetic signatures across multiple subsets. Bulk measurements of secreted proteins by standard enzyme linked immunosorbent assay (ELISA) are not capable of detecting these heterogeneities and the potential role of rare subsets in initiating an immune response². Furthermore, the effects of complex microenvironmental cues on cellular activation may be lost when only the average response of a population is examined. Therefore, in order to tease apart the various contributors to the functional variances among cells, we must be able to accurately assess their phenotype and function on a single cell level within controlled microenvironments.

Flow cytometry is the current gold standard for single cell analyses. However, similar to many other traditional molecular assays, cells are typically cultured in bulk and allowed to interact with one another and their external environment in an uncontrolled way. This type of methodology may overlook the effects of cell-cell paracrine interactions, which could only be revealed through single cell studies performed using

microwells. These methods are together necessary for a better understanding of cellular activation and function. Moreover, while flow cytometry combined with immunofluorescence and fluorescence in situ hybridization (FISH) has been used in phenotyping and genotyping single cells, functional assessment through measuring secreted products remain challenging. Protein transport inhibition followed by intracellular staining may be used, but disruption of protein transport can affect cellular functions including their adhesion and migration³. Enzyme-Linked ImmunoSpot (ELISPOT) has been developed for detection of secreted cytokines from single cells. In this method, cells are cultured on surfaces coated with capture antibody, localizing the signal to a “spot”. The ease with which actively secreting single cells can be enumerated has led to wide adoption of this assay in clinical settings⁴. However, cells are still cultured in bulk, and the adhesive microenvironment cannot be controlled since the surface underlying the cells is coated with capture antibody. In addition, it is difficult to quantify and correlate secreted products with individual cells, which has limited its usefulness in basic research.

As secreted proteins are central to cell-to-cell communication and coordinated immune responses, several recent technologies were developed to overcome the limitations of flow cytometry and ELISPOT by using microfabricated platforms. Love et al.⁵ first demonstrated a technique termed microengraving, which uses an array of microwells to physically isolate single cells. A glass substrate immobilized with capture antibodies covers the wells during cellular interrogation and is removed afterwards for analyte quantification by immunofluorescence. Subnanoliter wells present an attractive platform for single cell analyses as they completely eliminate paracrine signaling, provide

a uniform extracellular microenvironment across thousands of single cells, and are conducive to registrations of multiple measurements for each cell. By combining with an antibody barcode array detection strategy, the microwell platform has since been improved to allow simultaneous detection of 42 secreted proteins on a single cell level⁶. However, in both of these studies, the microwells were blocked with bovine serum albumin (BSA) prior to cell seeding to prevent cell adhesion. While these have been powerful tools in studying T cells⁷, B cells⁵, and circulating tumor cells⁸, which are non-adherent cells, they neglect the control of cell-matrix interactions that are important for adherent cells.

Macrophages are tissue-resident immune cells that play critical roles in development, metabolic regulation, maintenance of tissue homeostasis, and defense against invading pathogens. To carry out their diverse functions, macrophages must communicate and coordinate with both immune and non-immune cells, largely through their secretion of an impressive array of cytokines, chemokines and growth factors. While biochemical cues are thought to be the primary regulators of macrophage function, increasing evidence has surfaced to show that physical and adhesive microenvironmental cues can also affect macrophage phenotype and secretion⁹. For instance, extracellular matrix proteins fibronectin and fibrinogen have been shown to activate macrophage inflammatory pathways through Toll-like receptor 4 (TLR4)^{10,11}. In addition, physical features of biomaterial surfaces including substrate topography^{12,13} and rigidity¹⁴ are thought to modulate macrophage adhesion and activation. Our lab has previously shown that macrophage cell shape, specifically cell elongation, promotes an anti-inflammatory

phenotype¹⁵. Delineating the effects of these factors on macrophage cytokine secretion on a single cell level has not been possible with existing technologies described previously.

Here, we introduce a novel single cell analytical tool that allows for controlled physical microenvironment of single cells and simultaneous detection of their secreted products. The device combines three components in a sandwich format. The bottom level consists of an adhesive substrate with desired ECM proteins, and could potentially also incorporate topography or rigidity. The middle level is a thin PDMS membrane with arrays of microscale openings. By combining the bottom and middle layers, an array of microwells is formed. The PDMS membrane can be easily fabricated to contain openings of different shapes and sizes to control single cell shape and spreading¹⁶. The top level is a glass substrate that has been covalently conjugated with capture antibodies. A machined acrylic holder is used to fasten the three components together during cellular interrogation. Using this device, we demonstrate that ECM proteins and cell adhesion can affect macrophage secretion of inflammatory cytokines on a single cell level. We compared the single cell results with bulk cell measurements via enzyme-linked immunosorbent assays. We further show the unique capabilities of this platform by demonstrating an effect of cell shape on single macrophage secretion. Together, we validate this device as a powerful tool for studying the effect of physical and adhesive cues on cellular secretion at a single cell level.

Materials and Methods

Fabrication of microwells

Silicon wafers (University Wafer) containing 80- μm tall rectangular posts were fabricated using standard SU-8 photolithographic techniques. Briefly, SU-8 50 photoresist (MicroChem) was spin-coated onto a 3" silicon wafer, resulting in a uniform 80- μm thick layer. Following 2h of soft bake at 95 °C, the wafer was placed under a transparency mask containing clear rectangles (33 μm x 33 μm , 20 μm x 50 μm , or 10 μm x 100 μm) and exposed to UV light (AB&M UV Flood Lamp Exposure System) according to MicroChem protocol. After 10 minutes of post-exposure bake at 95 °C, the wafer was immersed in SU-8 developer for 5 minutes to rid of unpolymerized photoresist. Cleaned and dried wafer was baked at 200 °C for 30 minutes to allow the remainder SU-8 to completely crosslink. Finished wafers were silanized to facilitate replica molding.

PDMS (Dow Corning) was mixed at a 10:1 base-to-curing agent ratio and spin-coated onto silanized wafer at 1000 rpm for 1 minute to achieve a uniform thickness of 50 μm . PDMS support rings with an inner diameter of 12 mm were placed onto the wet wafer and cured with the membrane. The support rings allow easy removal of the 50- μm thick membrane from the wafer and subsequent handling and placement of the membrane. Sample cross sections of each batch of membranes were obtained, and the thickness of the membranes were confirmed to be within $50\pm 5\mu\text{m}$ using a microscope. The membranes were sterilized in 70% ethyl alcohol for 30 minutes, dried and stored at RT until use.

Sterile 18-mm glass coverslips were UV ozone treated for 15 min before adsorption with either 20 $\mu\text{g}/\text{mL}$ human fibronectin (BD Biosciences) or 2% Pluronic F-127 (Sigma Aldrich) for 1 h at room temperature (RT). After briefly drying with a nitrogen stream, 12-mm PDMS membranes and glass coverslips were exposed to UV

ozone for 15 min and then adhered together to form an array of microwells. Once the microwells were formed, the PDMS support rings were removed from the membranes. The microwells were incubated with a 2% Pluronic F-127 solution (Sigma Aldrich) at RT for 1 h while being desiccated to remove air bubbles from the wells. The microwells were rinsed thoroughly with PBS prior to cell seeding.

Modification of detection substrates

Standard 25 mm x 75 mm glass microscope slides were cleaned with concentrated H₂SO₄ and autoclaved in sterile pouches. Clean slides were wiped with isopropanol and UV ozone treated for 15 min. The slides were then silanized with a 4% (3-mercaptopropyl)trimethoxysilane solution (Sigma Aldrich) at RT for 1 h. Meanwhile, NeutrAvidin proteins were conjugated with sulfo-SMCC crosslinkers (both from Life Technologies) at RT for 30 min. Silanized glass slides were washed thoroughly with 100% ethanol and dried with N₂ stream. A clean silicone gasket of 10 milliwells (Grace Bio-labs) was sealed onto the slide for incubation of protein standards. The maleimide-activated NeutrAvidin was added to a 2 mL 7 kDa Zeba desalting column (Thermo Scientific) and centrifuged at 2000 rpm for 3 min to remove excess crosslinkers. The collected maleimide-activated NeutrAvidin was diluted to 10 µg/mL and incubated on the silanized slide at RT for 1 h. Following washing and blocking with 1% bovine serum albumin (BSA; MP Biomedicals) in PBS, the slides were incubated with 5 µg/mL of biotinylated LEAF purified capture antibodies (MCP-1: Clone 2H5; Biolegend) at 4°C

overnight. Prior to cytokine interrogation, the detection slides were washed and blocked with 1% BSA for 30 min at RT.

Cell seeding and cytokine interrogation

All protocols involving animals were approved by University of California Irvine's Institutional Animal Care and Use Committee, which is accredited by the Association for the Assessment and Accreditation of Laboratory Animal Care International (AAALACi). Bone marrow derived macrophages (BMDMs) were harvested from 6- to 12- week old female C57BL/6J mice (Jackson Laboratory). Briefly, bone marrow cells were flushed out of the femurs with DMEM supplemented with 3% heat-inactivated fetal bovine serum (HI FBS), and treated with ACK lysing buffer to remove red blood cells (all from Life Technologies). The remaining bone marrow cells were cultured in a macrophage differentiation media consisting of DMEM supplemented with 10% HI FBS, 1% penicillin/streptomycin, 2 mM L-glutamine, and 1% conditioned media containing macrophage colony stimulating factor (M-CSF). After 7 days, BMDMs were removed from culture using cell dissociation buffer (Life Technologies), seeded into the microwells, and then centrifuged at 700 rpm for 2 minutes to help the cells settle into the microwells. BMDMs were allowed to adhere and spread into the shapes of the microwells overnight. Immediately before cytokine interrogation, cells were stimulated with either 1 or 10 ng/mL lipopolysaccharide (LPS) and 10 ng/mL interferon- γ (IFN γ) (both from Biolegend), and stained with 2.5 μ g/mL of Hoechst 33342 (Life Technologies). The detection substrates were inverted over the microwells and sealed in a

homemade housing unit for the duration of cytokine interrogation. For the protein standard, the silicone gasket with 3 mm wells (Grace Bio-Labs) were loaded with known concentrations of recombinant mouse MCP-1 proteins (Biolegend). Upon completion of interrogation, cells sealed in the microwells were first imaged intact to obtain an accurate account of single cells in wells. Next, the detection substrates were gently removed, and the cells in the microwells were simultaneously stained with calcein-AM (green) and ethidium homodimer-1 (red) to differentiate live and dead cells, respectively. The detection substrates were washed with 1% BSA and stained with 5 $\mu\text{g}/\text{mL}$ of Oregon Green-conjugated anti-mouse MCP-1 (Clone 4E2; Biolegend).

Imaging and analysis

To identify regions on the detection coverslip corresponding to wells containing single cells, nuclei were labeled and imaged in intact devices. The nuclear image was captured by scanning the device using a 10x objective. Acquired tiles were stitched using the Grid/Collection Stitching plugin¹⁷ shipped with Fiji¹⁸ before analysis with custom software. Then, the detection coverslip was removed, processed, and imaged separately. Single cells were identified in the nuclear image and an affine transformation was computed to register single cells onto their corresponding region of the detection coverslip image. The detection substrates were scanned using a 40x oil-immersion objective to enhance detection limit. To correct for uneven illumination and background signal, the first-percentile intensity z-projection of the collected images was computed and subtracted from each image (with zero-truncation) before stitching. To compute an

affine mapping between the nuclear and detection images, at least 20 matching sets of landmarks were manually registered using ImageJ¹⁹. After mapping, measurement ROI locations for each single cell were polished by five rounds of iteratively updating the center of the ROI to the center of mass of the provisional ROI, which centered measurement ROIs on their matching well. Fluorescent images of the protein standards were similarly acquired, and the intensities were measured in ImageJ. A plot of fluorescence intensity vs. protein concentration was created. A linear regression line was plotted through the linear portion of the standard data points and was used to convert the intensities of cell secretion into concentrations of secreted proteins. All imaging was done on an Olympus IX83 inverted microscope equipped with an automated stage, using μ Manager control software²⁰. Our custom analysis software is available at <https://github.com/WendyLiuLab/elisascripts> under a MIT license. The secretion of at least 1000 single cells were measured for each experimental condition, and the secretion distribution of each experimental population is plotted in a density probability curve so that the distribution is normalized to the population size.

Bulk Macrophage Culture and Cytokine Secretion

6-well plates were coated with either fibronectin or pluronics prior to cell seeding. 500,000 BMDMs were seeded in each well with 2 mL of media. Cells were stimulated with either 1 ng/mL or 10 ng/mL LPS, and supernatants were collected at various time points for ELISA. ELISAs were carried out using mouse MCP-1 kits purchased from Biolegend and according to manufacturer's instructions. To compare single cell and bulk

culture secretion, average single cell secretions were adjusted for volume differential between single microwell and single tissue culture well (50 pL vs. 2 mL) and then multiplied by 500,000, the number of cells in each bulk culture well. The resultant sums of single cell secretions (Σ single cell) were directly compared to the bulk ELISA results.

Statistical Analysis

Data were presented as the mean \pm SEM across at least three independent experiments, unless otherwise specified. For single cell experiments under different soluble conditions and on different adhesive substrates, at least 1000 single cells from each experimental condition were examined. For single cell experiments under different cell shapes, at least 50 single cells from each experimental condition were examined. To establish statistical significance, two-tailed Student's *t*-tests were performed, and $p < 0.05$ was considered significant.

Results

Design of the microwell system

We employed a modular design for our single cell cytokine detection platform (Fig. 1). We started with a cell culture substrate, which can be any surface that supports cell adhesion. For our experiments, we used glass substrates adsorbed with ECM proteins. This design allows us to easily exchange the glass surface for other materials with either chemical or physical surface modifications in order to investigate the effects

of those modifications on cell behavior. The next component in the device is a 50 μm -thick PDMS membrane with micrometer-sized openings. The membrane is fabricated using standard photolithography and replica molding. PDMS was spin-coated onto silicon wafers containing 80 μm -tall posts to create a membrane with a uniform thickness of 50 μm . The posts can be designed to have cross sections of different shapes and sizes in order to control single cell shape and spread area.

Combining the cell culture substrate and the PDMS membrane with through holes together, an array of microwells was formed. The remainder areas of the microwell array was further blocked with Pluronic F127 to ensure that the cells only adhere to the bottom of the wells. The last component of the system is the detection substrate. To ensure maximal conjugation of capture antibodies and minimize signal background, the substrates were cleaned with an organic solvent and autoclaved, as steam has been shown to remove micro- and nano- topographical features on glass²¹. For conjugation of capture antibodies, we used a covalent conjugation strategy in which a glass surface is first functionalized with a mercaptosilane and subsequently allowed to react with NeutrAvidin proteins via an amine reactive maleimide moiety. Biotinylated capture antibodies were then bound to the NeutrAvidin proteins. When compared to direct adsorption of capture antibodies, this approach ensures higher stability and yield of antibodies on the glass surface²².

To combine all three components, the microwell arrays were inverted over the detection surface. Pressure was applied using an acrylic housing unit containing two plates screwed together to seal the wells against the detection substrate. To test the

system in its entirety, BMDMs were seeded into the microwells. Cells were stimulated with 10 ng/mL LPS and IFN γ and introduced to Hoechst nuclei stain prior to interrogation. The wells were sealed with a detection substrate conjugated with anti-MCP-1 capture antibody for 12 h. During this time, the acrylic housing unit was placed directly under the microscope and scanned for Hoechst signal to identify which wells contained only single cells (Fig. 2 a). Following interrogation, the detection substrate was removed from the housing unit and stained with a fluorescent detection antibody. Fluorescent micrographs of the detection substrate were taken using an 40x oil-immersion objective (Fig. 2 b), and the detection micrograph was correlated to the micrograph of cells in microwells (Fig. 2 c and d). To confirm the viability of the cells following interrogation, a time course experiment was conducted. At the end of 6 h, 12 h, and 24 h of interrogation, cells in the microwells were simultaneously stained with calcein-AM (green) and ethidium homodimer-1 (red) to differentiate live and dead cells, respectively (Fig. 2 e). The total viability of cells in microwells remained relatively constant (~80%) over the 24 h period, suggesting that the system is suitable for monitoring cell secretion over at least a 24 h period under incubated and humidified conditions.

A final feature we wanted to include in this device was absolute quantification of secreted proteins. On every detection substrate, we placed a silicone gasket with 3 mm circular openings to form an array of milliwells. In these wells, we loaded known concentrations of recombinant target proteins and incubated for the same amount of time as cell interrogation. The detection substrate was processed as previously described, and these protein standard wells were imaged the same way as cell secretion (Supp. Fig. 1 a).

Once we obtained the mean fluorescence intensity (MFI) at each protein concentration, we generated a standard curve to correlate the MFI from cell secretion experiments to protein concentration (Supp. Fig. 1 b). For MCP-1, a concentration of 1.25 ng/ml was near the limit, since the fluorescence levels achieved at this concentration were similar to background. Therefore, quantification of cells secreting below this lower limit is not possible using the current method.

Single macrophage secretion of MCP-1 under different soluble conditions

To validate our single cell cytokine detection platform, we first examined whether we can detect differences in secretion levels of cells under different levels of soluble stimuli. We stimulated the cells with 10 ng/ml of IFN- γ and 1 or 10 ng/ml of LPS. BMDMs were seeded into 33 x 33 μ m fibronectin-coated microwells. The cells were allowed to adhere and spread into the shape of the wells for 12 h, after which cells were stimulated and microwells were immediately sealed against detection substrates modified with anti-MCP-1 capture antibody. The activated cells were allowed to secrete MCP-1 for 6 h, and at least 1000 cells containing single cells were analyzed for each stimulation condition. Single cell secretion levels were graphed as a histogram to show population level heterogeneity (Fig. 3 a, left), as well as the cumulative distribution to directly compare the percentage of cells secreting over the detectable range of MCP-1 concentrations (Fig. 3 a, right). Baseline cell secretion levels from different mice varied significantly (Supp. Fig. 2), but we still observed higher average single cell secretion of MCP-1 under higher LPS stimulation, as expected (Fig. 3 b). Finally, we compared the

single macrophage secretion results to a standard bulk ELISA. The average concentration of single cell secretion from the single cell experiments was calculated, multiplied by 500,000 or the average the number of cells in each bulk culture well, and then adjusted for differences in volume in the microwell and bulk culture conditions. Interestingly, the sum of the single cell secretion (Σ single cell) was significantly less than that of bulk secretion. Although the same trend of increasing MCP-1 secretion with increasing LPS stimulation is observed, Σ single cell values were consistently 50 times less than bulk secretion (Fig. 3 c), suggesting that paracrine signaling may be involved in amplification of secretion when cells are cultured in bulk.

Single macrophage secretion of MCP-1 on different adhesive substrates

Next, we examined the effect of cell adhesion on cytokine secretion using our single cell device. We compared macrophages cultured on fibronectin-coated surfaces with macrophages cultured on non-adhesive Pluronics-coated surfaces, since we initially found that these two substrates led to the greatest difference in BMDM MCP-1 secretion in bulk assays (Supp. Fig. 3). In addition, we examined secretion every 6 h over an 18 h time period to reveal secretion dynamics. BMDMs were seeded into 33 x 33 μ m microwells coated with either fibronectin or Pluronics. The cells were allowed to adhere and spread into the shape of the wells for 12 h. Afterwards, cells were stimulated with 10 ng/mL LPS and 10 ng/mL IFN- γ and immediately sealed against detection substrates modified with MCP-1 capture antibody. The activated cells were interrogated for MCP-1 secretion for 6, 12, or 18 h. The secretion of at least 1000 cells were analyzed for each

experimental group. Representative probability distribution and cumulative distribution plots (Fig. 4 a) from one experiment are shown. As expected, the average population secretion levels increased with increasing time of interrogation. Consistent with bulk ELISA results, the experiments conducted in microwells showed that there was more MCP-1 secretion when BMDMs were cultured on fibronectin when compared to Pluronics (Fig. 4 b). This was not due to changes in cell viability since cells cultured on fibronectin and Pluronics are both equally viable (Supp. Fig. 4). In general, the probability distribution curves all have one tall peak signifying a large population of relatively low secreting cells. As shown in the cumulative distribution plot, the fibronectin curves generally have higher number of high secreting cells, which leads to higher average secretion level. Interestingly, the probability distribution curves for cells cultured on fibronectin displayed a wider and more spread out tail toward higher secretion levels. This was most noticeable at 18 h (Fig. 4 a, bottom left), which suggests that adhesion to ECM enhances the population of high secretors, and may contribute to population heterogeneity. This is further supported by the cumulative distribution curves, where the slope of the curve of cells on fibronectin is less steep than the curve of cells cultured on Pluronics, particularly at longer durations. Together these data suggest that adhesion to ECM may contribute to greater population heterogeneity.

We compared the single cell secretion levels with bulk ELISA results, and similar to previous experiments, we observed much lower secretion levels in the single cell experiments (Fig. 4 c). Interestingly, although we observed an increase in secretion of MCP-1 for cells cultured on fibronectin when compared to Pluronics, and higher levels at longer durations in both single and bulk experiments, the differences are more

pronounced in the single cell experiments. More specifically, in microwell experiments, the secretion of MCP-1 at 18 h is nearly three-fold higher than secretion at 6 h (Fig. 4 b). In contrast, in bulk culture condition, it appeared that most cytokine secretion is complete by 6 h, and the levels were only about 30 percent higher at 18 h (Fig. 4 c). This may be attributed to amplification of secretion by paracrine interactions, where large populations of cells together would more quickly reach saturating secretion levels. Together, these results show that our device is capable of detecting the effect of adhesion on single cell cytokine secretion, and also suggest that a device that can control cell adhesion, isolate individual cells, and simultaneously detect cell secretion may reveal previously undescribed cellular behaviors.

Single macrophage secretion of MCP-1 with different cell shape

Finally, we wanted to investigate the effect of cell shape on single macrophage secretion. This was in part motivated by our previous work, where we discovered that elongated cell morphology promoted macrophage polarization toward a more anti-inflammatory, alternatively activated phenotype¹⁵. We had previously controlled the shape of macrophages through micropatterning and examined their secretion using an ELISA-based cytokine array, but only discovered moderate decreases for a few inflammatory cytokines after engineered cell elongation. We had reasoned that cellular heterogeneity and the imperfect bulk method of controlling cell shape may have confounded our results. Using the newly developed single cell cytokine detection method where we can control single cell shape, we sought to re-address this important question.

We designed microwells with different shapes but all with the same area of $1000 \mu\text{m}^2$, which was the average area of a spread macrophage determined in our previous study. This allowed us to eliminate cell area as a potential factor that could influence cell secretion. To investigate cell elongation, we chose three different aspect ratios or elongation factors: 1, 2.5, and 10. We designed these three types of microwells, which have the dimensions of $33 \times 33 \mu\text{m}$, $20 \times 50 \mu\text{m}$, and $10 \times 100 \mu\text{m}$ (Fig. 5 a, top). By simply seeding single BMDM macrophages into these wells and allowing them to spread into the shape of the wells, we demonstrated that we could control single cell shape and area (Fig. 5 a, bottom). Once the cells assumed the shape of the wells, they were stimulated with 10 ng/mL each of LPS and $\text{IFN-}\gamma$ and the wells were immediately sealed with detection substrates modified with anti-MCP-1 capture antibody. After 6 h of cytokine interrogation, single cells from each shape condition were analyzed for their MCP-1 cytokine secretion (Fig. 5 b-d). Interestingly, the most elongated macrophages, cultured in microwells with 1:10 aspect ratio ($10 \times 100 \mu\text{m}$), secreted significantly less inflammatory cytokine MCP-1 than the other cell shapes (Fig. 5 d). This corroborates our previous finding that elongation of macrophages protect cells from inflammatory activation. Although the $33 \times 33 \mu\text{m}$ macrophages appeared to secrete less MCP-1 than $20 \times 50 \mu\text{m}$ macrophages, the difference was much less than that between $33 \times 33 \mu\text{m}$ and $10 \times 100 \mu\text{m}$ cells. This result supports our previous study, where patterning macrophages on $50 \mu\text{m}$ -wide lines (leading to approximately a $20 \times 50 \mu\text{m}$ cell shape), did not significantly affect macrophage activation. This result is also interesting in that when we examined MCP-1 secretion in bulk micropatterned cells, we did not observe any statistically significant changes in secretion between elongated and non-elongated cells¹⁵.

However, with our single cell cytokine detection device, differences in cell secretion based on cell shape were detected, which could not be detected in traditional bulk assays, further signifying the usefulness and necessity of this device.

Discussion

In this work, we used microfabrication techniques to create arrays of microwells that contained ECM-coated adhesive bottoms. Recent work on single cell secretion have used microarrayed wells for cell isolation, and immunofluorescence-based sandwich assays for detection of secreted product^{5,6}. While this has been a revolutionary tool for studying nonadhesive cells including T cells and B cells, it was not capable of controlling the adhesive microenvironment, important for many cell types including macrophages. Motivated by our previous work, where we demonstrated the importance of adhesion and cell morphology on macrophage activation, we sought to develop a platform to assess single cytokine secretion while controlling individual cell adhesion and geometry. By manipulating the microwell size and geometry, we controlled single macrophage morphology and spreading. Macrophage viability in the microwells remained relatively constant over a 24-hour period, which makes this a practical platform for monitoring single cell secretion dynamics over time.

We validated our system by first examining single macrophage secretion of inflammatory cytokine MCP-1 under different levels of soluble stimuli. As expected, higher doses of LPS resulted in elevated secretion of MCP-1, which was supported by bulk ELISA tests. However, unlike ELISA, we were able to detect varying overall

averages as well as individual cell distributions, the latter of which revealed a subset of high-secreting cells within the population. Although our device could not quantify a fraction of the population that were secreting at levels below the detection limit, it would likely be possible to detect secretion levels of all cells if higher cytokine stimulation levels or longer interrogation times were used. Continued work will focus on enhancing detection sensitivity with advanced imaging tools and improved molecular probes in order to better quantify the entire population including low secreting cells.

We further used this single cell platform to examine the effect of different adhesive substrates, a novel capability of our device. Consistent with bulk ELISA data, we observed higher single macrophage secretion of MCP-1 on fibronectin than Pluronics. Furthermore, while the average single macrophage secretion on pluronics increased with increasing duration of interrogation, the secretion profiles retained relatively similar shapes over the same time course. However, macrophages cultured on fibronectin exhibited higher levels of secretion heterogeneity over that time period, suggesting that adhesion to ECM proteins may be in part responsible for cellular heterogeneity. Interestingly, the average single cell secretion in microwells was significantly lower when compared to measurements from bulk ELISA experiments. This suggests the presence of paracrine signaling in bulk cultures likely amplifies the overall population secretion, which is consistent with previous studies of macrophages in microwells where paracrine signals were revealed to be important for coordinating their response to TLR4 ligands²³. This is also supported by recent work suggesting that a few precocious cells that express high levels of inflammatory cytokines at early times are important for

regulating the population response²⁴. Indeed, our studies also reveal population heterogeneity and high secreting cells at early time points.

Finally, we used our device to examine the effect of macrophage cell shape on single cell secretion, which was the ultimate motivation behind developing this device. We restricted cell area to $1000 \mu\text{m}^2$ while varying aspect ratio from 1:1 to 1:10. Intriguingly, single macrophage secretion of MCP-1 correlated with cell aspect ratio. The most elongated single macrophages, assuming the 1:10 aspect ratio, secreted the least amount of MCP-1, whereas the roundest macrophages (1:1) secreted the most MCP-1. This not only supports our previous finding that macrophage elongation promotes a more anti-inflammatory phenotype, it also directly links cell shape with macrophage function. More importantly, this reduction in secretion was not observed in bulk measurements, and was only possible due to the development of this single cell platform.

The inherent heterogeneity of cell populations is increasingly being recognized as a key driver of population behavior, but progress in understanding the underlying phenomena has been hindered by the limitations of traditional bulk assays. Recent advances in single cell RNA-sequencing has revealed unique information that cannot be obtained with traditional methods, and demonstrated a critical role of cellular heterogeneity in controlling population level response²⁴. In this light, there has been increasing demand for single cell technologies. While techniques to evaluate single cell protein biomarkers (flow cytometry) and gene expression (RNA-seq) has already been established, one area that has proven difficult to advance has been secreted products. These are arguably the most important for coordinating population level response as they facilitate cell-to-cell communication. Also, measuring secreted proteins directly rather

than mRNA copies has distinct advantages. Proteins and mRNA content within a cell are not necessarily correlated, especially when measurements are taken in static snapshots. Moreover, both are subject to intrinsic and extrinsic stochasticity, including different rates of production (transcription or translation) and degradation²⁵. Specifically in the case of immune cells, inflammatory cytokines such as IL-1 β and the mRNAs of inflammatory cytokines such as TNF α are often produced in advance and stored within cells²⁶. Such design enables these cytokines to be rapidly released upon stimulation, which is why we could observe macrophage secretion of these proteins within thirty minutes of stimulation. Therefore, measuring secreted proteins from single cells provides a more accurate functional assessment of how each cell may be affecting the entire population.

Conclusions

We have developed a novel single cell secretion analysis platform that allows for precise control of cell adhesion and shape. The results obtained thus far using this device clearly demonstrate effects of adhesive cues on macrophage secretion that would not be detected otherwise, substantiating the potential impact it may have on the study of adherent cells. Clearly, much work remains to be done to explore these initial findings. For instance, it will be interesting to tease apart the potential paracrine signaling effect, which can be performed using microwells that contain pairs or even larger numbers of cells. Our platform can be used to compare the secretion of single cells versus multiple cells, where the shape and area of each cell and the degree of cell-cell contact are kept

constant^{27,28}. Furthermore, improving detection sensitivity using advanced imaging methods or alternative molecular probes would make it possible to evaluate low secreting cells, or even interrogate the effects of cell shape without cytokine stimulation. The tool further allows for the study of other adherent cell types^{29,30}, including stem cells, tumor cells, epithelial or endothelial cells, among many others, in which secreted products may be critical for a coordinated response within tissues.

Acknowledgements

This work was supported by the National Institutes of Health (NIH) National Institute of Dental and Craniofacial Research (NIDCR) DP2DE023319 and the Interdisciplinary Innovation Initiative in the Henry Samueli School of Engineering at the University of California Irvine. F.Y.M. was supported by a NIH T32 Systems Biology of Development Training Fellowship. T.D.S. is supported by the National Science Foundation (NSF) Graduate Research Fellowship Program (DGE-1321846). T.U.L. is supported by a California Institute of Regenerative Medicine (CIRM) Training Fellowship (TG2-01152). The authors acknowledge the ggplot³¹, R³², and scipy³³ projects for their helpful tools, which were used in the preparation of this manuscript.

References

- 1 P. K. Chattopadhyay, T. M. Gierahn, M. Roederer and J. C. Love, *Nat. Immunol.*, 2014, **15**, 128–35.

- 2 A. Yalçın, Y. J. Yamanaka and J. C. Love, *Methods Mol. Biol.*, 2012, **853**.
- 3 A. D. Bershadsky and A. H. Futerman, *Proc. Natl. Acad. Sci.*, 1994, **91**, 5686–5689.
- 4 M. Slota, J.-B. Lim, Y. Dang and M. L. Disis, *Expert Rev. Vaccines*, 2011, **10**, 299–306.
- 5 J. C. Love, J. L. Ronan, G. M. Grotenbreg, A. G. van der Veen and H. L. Ploegh, *Nat. Biotechnol.*, 2006, **24**, 703–7.
- 6 Y. Lu, Q. Xue, M. R. Eisele, E. S. Sulistijo, K. Brower, L. Han, E. D. Amir, D. Pe'er, K. Miller-Jensen and R. Fan, *Proc. Natl. Acad. Sci.*, 2015, 201416756.
- 7 Q. Han, N. Bagheri, E. M. Bradshaw, D. A. Hafler, D. A. Lauffenburger and J. C. Love, *Proc. Natl. Acad. Sci.*, 2012, **109**, 1607–1612.
- 8 X. Yao, A. D. Choudhury, Y. J. Yamanaka, V. a Adalsteinsson, T. M. Gierahn, C. a Williamson, C. R. Lamb, M.-E. Taplin, M. Nakabayashi, M. S. Chabot, T. Li, G.-S. M. Lee, J. S. Boehm, P. W. Kantoff, W. C. Hahn, K. D. Wittrup and J. C. Love, *Integr. Biol. (Camb)*, 2014, **6**, 388–98.
- 9 F. Y. McWhorter, C. T. Davis and W. F. Liu, *Cell. Mol. Life Sci.*, 2014, **72**, 1303–1316.
- 10 Y. Okamura, M. Watari, E. S. Jerud, D. W. Young, S. T. Ishizaka, J. Rose, J. C. Chow and J. F. Strauss, *J. Biol. Chem.*, 2001, **276**, 10229–33.
- 11 S. T. Smiley, J. A. King and W. W. Hancock, *J. Immunol.*, 2001, **167**, 2887–2894.
- 12 S. Chen, J. A. Jones, Y. Xu, H. Y. Low, J. M. Anderson and K. W. Leong, *Biomaterials*, 2010, **31**, 3479–3491.
- 13 T. U. Luu, S. C. Gott, B. W. K. Woo, M. P. Rao and W. F. Liu, *ACS Appl. Mater.*

- Interfaces*, 2015, **7**, 28665–28672.
- 14 A. K. Blakney, M. D. Swartzlander and S. J. Bryant, *J. Biomed. Mater. Res. A*, 2012, **100**, 1375–86.
- 15 F. Y. McWhorter, T. Wang, P. Nguyen, T. Chung and W. F. Liu, *Proc. Natl. Acad. Sci. U. S. A.*, 2013, **110**, 17253–8.
- 16 E. Ostuni, R. Kane, C. S. Chen, D. E. Ingber and G. M. Whitesides, *Langmuir*, 2000, **16**, 7811–7819.
- 17 S. Preibisch, S. Saalfeld and P. Tomancak, *Bioinformatics*, 2009, **25**, 1463–5.
- 18 J. Schindelin, I. Arganda-Carreras, E. Frise, V. Kaynig, M. Longair, T. Pietzsch, S. Preibisch, C. Rueden, S. Saalfeld, B. Schmid, J.-Y. Tinevez, D. J. White, V. Hartenstein, K. Eliceiri, P. Tomancak and A. Cardona, *Nat. Methods*, 2012, **9**, 676–682.
- 19 C. a Schneider, W. S. Rasband and K. W. Eliceiri, *Nat. Methods*, 2012, **9**, 671–675.
- 20 A. Edelstein, N. Amodaj, K. Hoover, R. Vale and N. Stuurman, *Curr. Protoc. Mol. Biol.*, 2010, 1–17.
- 21 G. Wittenburg, G. Lauer, S. Oswald, D. Labudde and C. M. Franz, *J. Biomed. Mater. Res. A*, 2014, **102**, 2755–66.
- 22 J. H. Seo, L.-J. Chen, S. V Verkhoturov, E. a Schweikert and A. Revzin, *Biomaterials*, 2011, **32**, 5478–88.
- 23 Q. Xue, Y. Lu, M. R. Eisele, E. S. Sulistijo, N. Khan, R. Fan and K. Miller-Jensen, *Sci. Signal.*, 2015, **8**, ra59.
- 24 A. K. Shalek, R. Satija, J. Shuga, J. J. Trombetta, D. Gennert, D. Lu, P. Chen, R.

- S. Gertner, J. T. Gaublomme, N. Yosef, S. Schwartz, B. Fowler, S. Weaver, J. Wang, X. Wang, R. Ding, R. Raychowdhury, N. Friedman, N. Hacohen, H. Park, A. P. May and A. Regev, *Nature*, 2014, **509**, 363–9.
- 25 Y. Taniguchi, P. J. Choi, G.-W. Li, H. Chen, M. Babu, J. Hearn, A. Emili and X. S. Xie, *Science*, 2010, **329**, 533–538.
- 26 S. Carpenter, E. P. Ricci, B. C. Mercier, M. J. Moore and K. a Fitzgerald, *Nat. Rev. Immunol.*, 2014, **14**, 361–76.
- 27 C. M. Nelson and C. S. Chen, *FEBS Lett.*, 2002, **514**, 238–242.
- 28 W. F. Liu, C. M. Nelson, D. M. Pirone and C. S. Chen, *J. Cell Biol.*, 2006, **173**, 431–41.
- 29 W. Zhao, S. Schafer, J. Choi, Y. J. Yamanaka, M. L. Lombardi, S. Bose, A. L. Carlson, J. A. Phillips, W. Teo, I. A. Droujinine, C. H. Cui, R. K. Jain, J. Lammerding, J. C. Love, C. P. Lin, D. Sarkar, R. Karnik and J. M. Karp, *Nat Nanotechnol*, 2011, **6**, 524–531.
- 30 M.-C. Liao, C. R. Muratore, T. M. Gierahn, S. E. Sullivan, P. Srikanth, P. L. De Jager, J. C. Love and T. L. Young-Pearse, *J. Neurosci.*, 2016, **36**, 1730–1746.
- 31 H. Wickham, *ggplot2: elegant graphics for data analysis*, Springer Science & Business Media, 2009.
- 32 R. R Development Core Team, *R Found. Stat. Comput.*, 2011, **1**, 409.
- 33 T. E. Oliphant, *Comput. Sci. Eng.*, 2007, **9**, 10–20.

Figure Captions

Figure 1. Schematic of the single adherent cell cytokine detection platform.

Microwell system contains a PDMS gasket, an ECM-coated cell culture substrate, and a detection substrate coated with capture antibody. Secreted proteins are captured during the assay, and then measured using fluorescent detection antibodies.

Figure 2. Implementation of the single adherent cell cytokine detection system. (a)

Representative fluorescence image of Hoechts 33342-stained nuclei of cells cultured within an array of PDMS microwells. Single cells are outlined in red. Scale bar: 100 μm . **(b)** Representative fluorescence image of detection substrate probed with a fluorescent detection antibody after assay. Spots corresponding to the single cells in (a) are outlined in blue. **(c) and (d)** Magnified view of areas depicted in yellow boxes of (a) and (b), respectively. Scale bar: 50 μm . **(e)** Representative live/dead stain of cells after 24 h of interrogation in the microwell system (top) and quantification of cell viability (bottom).

Figure 3. Microwell platform detects changes in macrophage cytokine secretion upon simulation with different amounts of LPS. (a)

Probability density (left) and cumulative distribution (right) graphs of macrophages treated with 10 ng/ml IFN- γ and 1 or 10 ng/ml of LPS. **(b)** Quantification of relative mean MCP-1 secretion by individual

macrophages in (a) averaged across three separate experiments. (c) Quantification of absolute MCP-1 secretion by macrophages, summed across 500,000 cells for microwell experiments or bulk cultures containing 500,000 cells, averaged across three separate experiments. * denotes $p < 0.05$ when compared to 1 n/gml LPS stimulation condition in (b) or when compared to microwell culture with the same stimulation condition in (c).

Figure 4. Macrophage cytokine secretion is dependent on adhesive surface. (a) Representative probability density (left) and cumulative distribution (right) graphs of macrophages cultured on Pluronics or fibronectin for 6 (top), 12 (middle) or 18 h (bottom). (b) Quantification of relative mean MCP-1 secretion by individual macrophages shown in (a), averaged across three separate experiments. (c) Quantification of absolute MCP-1 secretion by macrophages summed across 500,000 cells for microwell experiments, or bulk cultures containing 500,000 cells, averaged across three separate experiments. * denotes $p < 0.05$ when compared to cells cultured on Pluronics at the same time point in (b) or when compared to microwell culture with the same stimulation condition in (c). # denotes $p < 0.05$ when compared to cells cultured in bulk on Pluronics at the same time point.

Figure 5. Macrophage elongation inhibits secretion of MCP-1. (a) Representative brightfield images of PDMS microwells with the indicated dimensions (top) and fluorescent images of macrophages cultured in microwells and probed with phalloidin to detect actin (in red) and Hoechts 33342 to detect nuclei (in blue) (bottom). Scale bars: 50 μm . (b) Representative fluorescent images of cell nuclei detected by Hoechts 33342 with

single cells outlined in red (top) and fluorescently labelled anti-MCP-1 on the detection substrate with single cells outlined in blue (bottom). Scale bars: 50 μm . **(c)** Representative probably density curve (left) and cumulative distribution curve (right) of MCP-1 secretion by macrophages cultured in different shaped microwells and stimulated with 10 ng/ml each of LPS and IFN- γ . **(d)** Quantification of average relative mean MCP-1 secretion by individual macrophages shown in (a), across three separate experiments. * denotes $p < 0.05$ when compared to cells cultured in 33 x 33 μm^2 microwells.

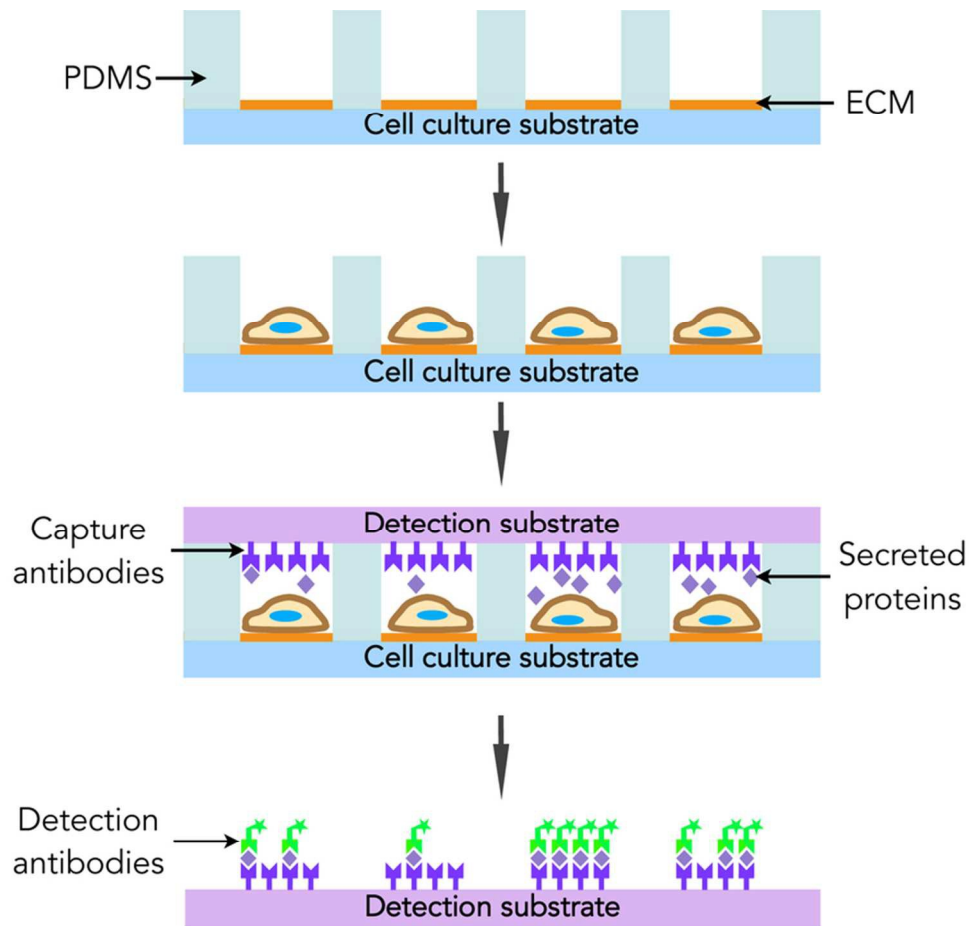


Figure 1. Schematic of the single adherent cell cytokine detection platform. Microwell system contains a PDMS gasket, an ECM-coated cell culture substrate, and a detection substrate coated with capture antibody. Secreted proteins are captured during the assay, and then measured using fluorescent detection antibodies.

77x72mm (300 x 300 DPI)

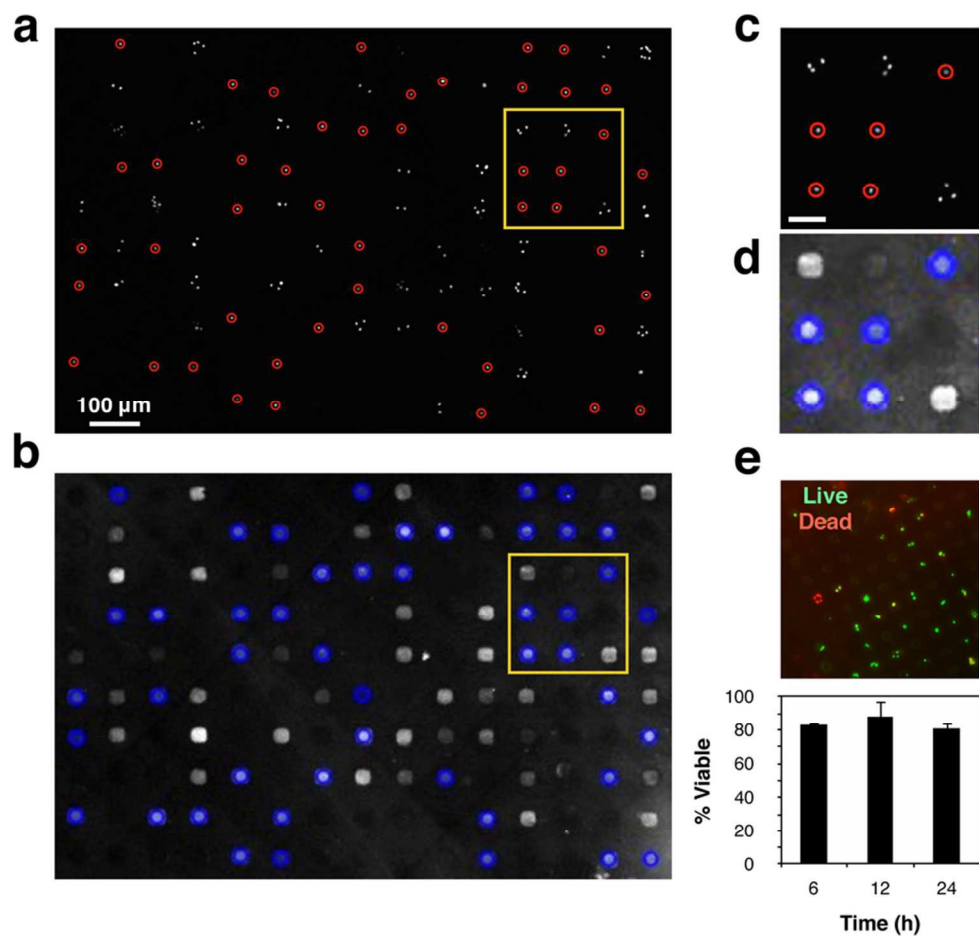


Figure 2. Implementation of the single adherent cell cytokine detection system. (a) Representative fluorescence image of Hoechts 33342-stained nuclei of cells cultured within an array of PDMS microwells. Single cells are outlined in red. Scale bar: 100 μm . (b) Representative fluorescence image of detection substrate probed with a fluorescent detection antibody after assay. Spots corresponding to the single cells in (a) are outlined in blue. (c) and (d) Magnified view of areas depicted in yellow boxes of (a) and (b), respectively. Scale bar: 50 μm . (e) Representative live/dead stain of cells after 24 h of interrogation in the microwell system (top) and quantification of cell viability (bottom).
79x76mm (300 x 300 DPI)

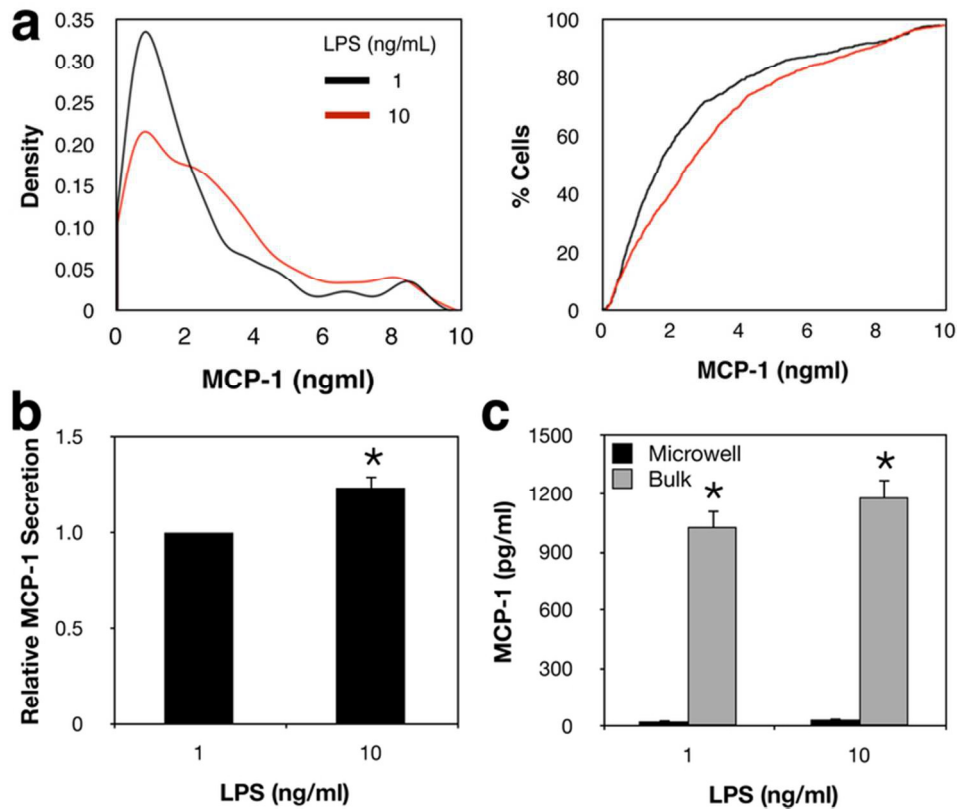


Figure 3. Microwell platform detects changes in macrophage cytokine secretion upon stimulation with different amounts of LPS. (a) Probability density (left) and cumulative distribution (right) graphs of macrophages treated with 10 ng/ml IFN- γ and 1 or 10 ng/ml of LPS. (b) Quantification of relative mean MCP-1 secretion by individual macrophages in (a) averaged across three separate experiments. (c) Quantification of absolute MCP-1 secretion by macrophages, summed across 500,000 cells for microwell experiments or bulk cultures containing 500,000 cells, averaged across three separate experiments. * denotes $p < 0.05$ when compared to 1 ng/ml LPS stimulation condition in (b) or when compared to microwell culture with the same stimulation condition in (c).

70x59mm (300 x 300 DPI)

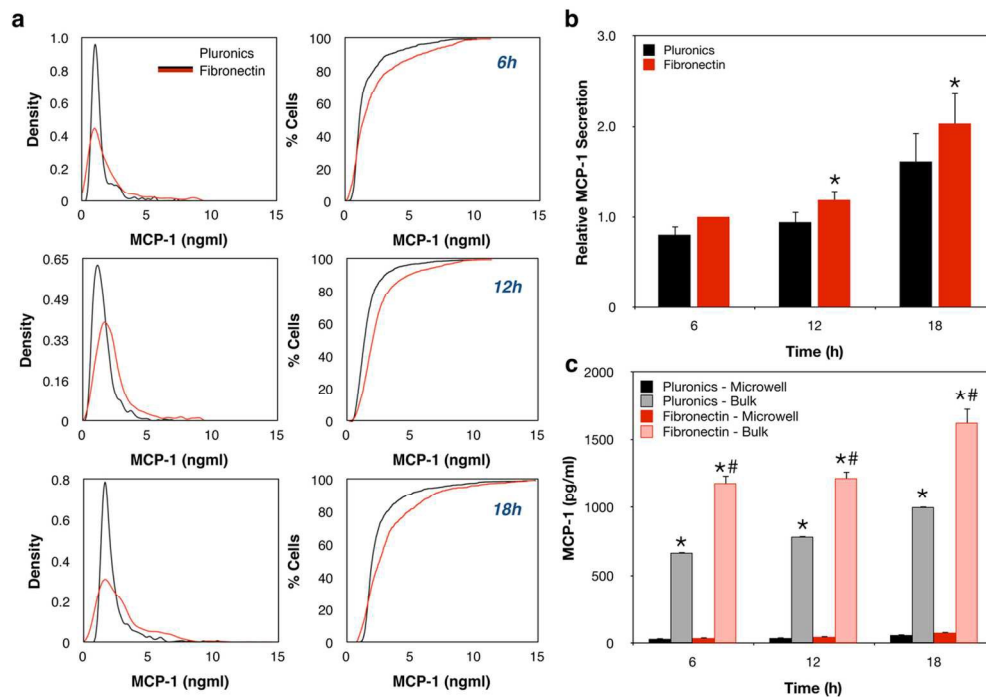


Figure 4. Macrophage cytokine secretion is dependent on adhesive surface. (a) Representative probability density (left) and cumulative distribution (right) graphs of macrophages cultured on Pluronic or fibronectin for 6 (top), 12 (middle) or 18 h (bottom). (b) Quantification of relative mean MCP-1 secretion by individual macrophages shown in (a), averaged across three separate experiments. (c) Quantification of absolute MCP-1 secretion by macrophages summed across 500,000 cells for microwell experiments, or bulk cultures containing 500,000 cells, averaged across three separate experiments. * denotes $p < 0.05$ when compared to cells cultured on Pluronic at the same time point in (b) or when compared to microwell culture with the same stimulation condition in (c). # denotes $p < 0.05$ when compared to cells cultured in bulk on Pluronic at the same time point.

120x84mm (300 x 300 DPI)

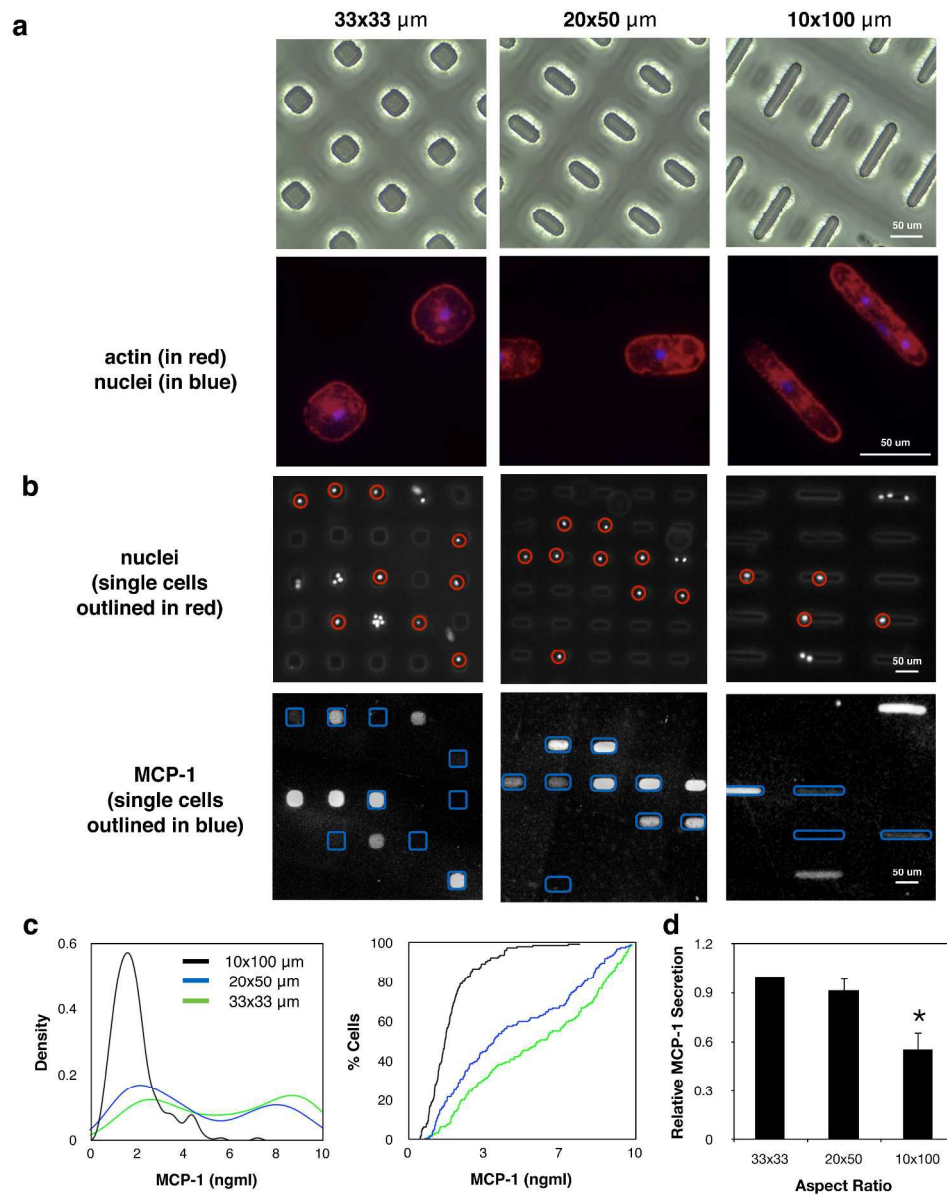


Figure 5. Macrophage elongation inhibits secretion of MCP-1. (a) Representative brightfield images of PDMS microwells with the indicated dimensions (top) and fluorescent images of macrophages cultured in microwells and probed with phalloidin to detect actin (in red) and Hoechts 33342 to detect nuclei (in blue) (bottom). Scale bars: 50 μm . (b) Representative fluorescent images of cell nuclei detected by Hoechts 33342 with single cells outlined in red (top) and fluorescently labelled anti-MCP-1 on the detection substrate with single cells outlined in blue (bottom). Scale bars: 50 μm . (c) Representative probability density curve (left) and cumulative distribution curve (right) of MCP-1 secretion by macrophages cultured in different shaped microwells and stimulated with 10 ng/ml each of LPS and IFN- γ . (d) Quantification of average relative mean MCP-1 secretion by individual macrophages shown in (a), across three separate experiments.

* denotes $p < 0.05$ when compared to cells cultured in 33 x 33 μm^2 microwells.
302x374mm (300 x 300 DPI)

Graphical and Textual Abstract

A microwell system for detection of secreted products from adherent cells is used to demonstrate that macrophage adhesive context and cell shape regulate cytokine secretion and population heterogeneity.

